

Nicotine induces a dual effect on the beige-like phenotype in adipocytes

Hui-jian Chen¹, Jie Xiang², Wan-xia Zhang¹, Ao Sun¹, Gai-ling Li¹ and You-e Yan^{1,*}

¹Department of Pharmacology, Wuhan University School of Basic Medical Sciences, 185, DongHu Road, Wuhan, China 430071

²Clinical Laboratory of Wuhan Medical Treatment Center, 1, Yintan Road, Wuhan, China, 430023

*Corresponding author: yanyoue@whu.edu.cn

Received: April 3, 2019; Revised: June 10, 2019; Accepted: June 14, 2019; Published online: July 6, 2019

Abstract: Nicotine, the main component of cigarette smoke, affects white/brown adipocytes. Few studies have concentrated on beige adipocytes. In this study, 3T3-L1 cells were differentiated in the presence of nicotine (25, 50 and 100 $\mu\text{mol/L}$) during early differentiation and maintenance stages. Cell viability and the state of lipid droplets were assessed by the MTT assay and Oil Red O, respectively, and the expression of beige-related genes and proteins was examined by RT-qPCR, Western blotting and flow cytometry. Nicotine did not alter adipocyte differentiation; however, it increased the expression of peroxisome proliferator-activated receptor gamma (PPAR γ) protein during early differentiation and maintenance. Nicotine treatment during early differentiation downregulated gene and protein expression of PPAR γ coactivator 1-alpha (PGC-1 α), uncoupling protein 1 (UCP1) and cluster of differentiation 137 (CD137), and gene expression of Cbp/p300 interacting transactivator with Glu/Asp rich carboxy-terminal domain 1 (Cited1), transmembrane protein 26 (Tmem26), and short stature homeobox 2 (Shox2). Nicotine treatment during the maintenance stage upregulated these beige-related genes/proteins. Nicotine treatment of immature adipocytes damaged beige function through a decrease in PGC-1 α /UCP1 expression, but nicotine treatment of mature adipocytes or both immature and mature cells enhanced beige functioning. Nicotine induced beige-like phenotype dysfunction in 3T3-L1 adipocytes. This process may affect thermogenesis in adipose tissue and cause a dysfunction in fat metabolism.

Keywords: nicotine; beige adipocytes; beige-like dysfunction; different differentiation stages; 3T3-L1

INTRODUCTION

Cigarette smoke is a traditional indoor air pollutant in our living environment. According to the investigation of the World Health Organization (WHO) from 2017, there were 1.1 billion smokers in the world, and around 80% of them were from low- and middle-income countries. Secondhand smoking and/or maternal smoking exposure in pregnancy also widely exist in children's living environments [1]. Nicotine is the main component of cigarette smoke, and it has multiple effects on endocrine organs, such as adipose tissue. For example, increased white fat and adipogenesis have been observed in nicotine-exposed prenatal rats [2]. In addition, direct nicotine exposure has been shown to reduce adipose weight, adipocyte size, and to induce adipose tissue triglyceride lipolysis [3]. However, the underlying mechanisms are still not fully understood.

Adipose tissue is an endocrine organ that participates in energy storage and regulates energy homeo-

stasis. Adipose tissue can be divided into white adipose tissue (WAT) and classical brown adipose tissue (BAT). WAT is responsible for energy storage in the form of triglycerides. BAT consumes energy, maintains body temperature and increases body energy expenditure via non-shivering thermogenesis [4]. In WAT, a new kind of adipocyte, with multilocular lipid droplet morphology and a higher mitochondrial content and expression of UCP1 as compared to white adipocytes, has been observed [5]. These special adipocytes, called beige adipocytes, can be found in WAT, but they show similar functions to brown adipocytes. When exposed to cold temperature or a β -adrenergic receptor agonist, UCP1 expression in beige adipocytes is activated by PGC-1 α . Nicotine plays an important role in regulating different types of adipose tissue. For example, maternal nicotine exposure can lead to increased visceral WAT in rat offspring [6], and direct nicotine exposure can induce the expression of uncoupling protein 1 (UCP1) in the BAT of 6-month-old obese mice [7]. However, only a

few studies have focused on the effects of nicotine on beige adipocytes. It can be speculated that nicotine also affects the functions (e.g. thermogenesis ability and cell quantity) of beige adipocytes.

The 3T3-L1 cell line is a well-established preadipocyte line [8], and it is widely used in adipocyte-related *in vitro* studies [9,10]. However, there has been no study focused on the effect of nicotine on beige adipocytes in the 3T3-L1 cells. Related research has confirmed the ability of the 3T3-L1 cell line to express beige-related genes [11]. The 3T3-L1 cell line was chosen in our study to explore the effects of nicotine on beige adipocytes at different differentiation stages. In addition, *Ucp1* is an important thermogenesis-specific gene of beige adipocytes, and the protein expression of peroxisome proliferator-activated receptor gamma coactivator 1-alpha (PGC-1 α) could induce the expression of UCP1 and other thermogenic components [12]. In our study, the thermogenesis ability of beige adipocytes was evaluated via examination of the expression of PGC-1 α and UCP1. Cluster of differentiation 137 (*Cd137*), transmembrane protein 26 (*Tmem26*), T-box transcription factor 1 (*Tbx1*), Cbp/p300 interacting transactivator with Glu/Asp rich carboxy-terminal domain 1 (*Cited1*), short stature homeobox 2 (*Shox2*) and homeobox C9 (*Hoxc9*) are usually identified as beige-specific makers [7,13,14], which contributed towards the identification of the amount of beige adipocytes. It is reported here for the first time that nicotine acts on beige adipocytes.

MATERIALS AND METHODS

Chemicals

3T3-L1 preadipocytes were obtained from the Cell Bank of Type Culture Collection of the Chinese Academy of Sciences. Nicotine, penicillin-streptomycin, insulin, dexamethasone, 3-isobutyl-1-methylxanthine and Oil Red O were purchased from Sigma (USA); high glucose Dulbecco's modified Eagle's medium (DMEM) and fetal bovine serum (FBS) were purchased from Gibco (USA); TRIzol reagent and anti-mouse CD137-APC antibody were obtained from Invitrogen (USA); SYBR Green and the reverse transcriptase kit were purchased from Takara (China); the anti-UCP1 antibody, anti-PGC-1 α antibody and anti-glyceraldehyde-3-phosphate dehydrogenase (GAPDH) antibody

were obtained from Abcam (USA); anti-peroxisome proliferator-activated receptor gamma (PPAR γ) antibody was obtained from Bioss (China).

Cell culture and differentiation

3T3-L1 mouse embryo fibroblasts were maintained in DMEM supplemented with 10% FBS until confluent and then in the same medium for another 2 days. The first stage of differentiation (days 0-2) was maintained for 2 days by adding differentiation media I: 10 μ g/mL insulin, 1 μ mol/L dexamethasone and 0.5 mM 3-isobutyl-1-methylxanthine (IBMX) in DMEM with 10% FBS. During the second stage (days 3-4), the culture medium was replaced by differentiation media II: DMEM containing 10% FBS and 10 μ g/mL insulin. Finally, cells were maintained in DMEM with 10% FBS for 6 days (days 5-10) before harvesting. Nicotine treatment (25, 50, and 100 μ mol/L) was supplemented during the early differentiation stage (Group 1, days 0-4), maintenance stage (Group 2, days 5-10) and the entire 10-day period (Group 3, days 0-10).

Cell viability

3T3-L1 preadipocytes were seeded onto 96-well plates at a density of 10^3 cells/cm² and cultured in the presence of 10^{-1} - 10^5 μ mol/L nicotine for 24, 48 and 72 h (n=8). The cells were treated with MTT assay reagents (1 mg/mL) for 4 h and the resulting formazan was solubilized in 150 μ L dimethyl sulfoxide (DMSO). The absorbance was measured at 570 nm.

Oil Red O staining

The 3T3-L1 cells were washed twice with phosphate-buffered saline (PBS) and fixed with neutral formaldehyde, then washed rapidly with 60% isopropanol. The cells were incubated with Oil Red O solution (0.6% Oil Red O dye in isopropanol and water at a 3:2 ratio) for 20 min. Finally, the samples were washed rapidly with 60% isopropanol and then washed three times with deionized water. Images were captured with a microscope. For quantitative analysis, 500 μ L/well isopropanol were added into 12-well plates to dissolve the Oil Red O in the lipid droplets, and the liquid was then transferred to a 96-well plate. The absorbance was measured at 570 nm.

Real-time quantitative PCR (RT-qPCR)

The total cellular RNA was obtained by TRIzol Reagent. One μg RNA was converted to cDNA using a reverse transcriptase kit. In the quantitative real-time polymerase chain reaction (RT-qPCR) analysis, the relative expression levels of genes were quantified using SYBR Green with ribosomal protein, P0 (*36b4*) as a housekeeping gene. The RT-qPCR was conducted using a CFX connect machine (Bio-Rad, USA), and the genes were analyzed using the $\Delta\Delta\text{CT}$ method. The sequences of the primer sets used in this study are listed in Supplementary Table S1.

Western blot analysis

The 3T3-L1 adipocytes were harvested and lysed in ice-cold radioimmunoprecipitation assay (RIPA) lysis buffer for 30 min. The protein content was tested using a bicinchoninic acid (BCA) kit and all samples were adjusted to the same concentration. The protein samples were separated by 12% sodium dodecyl sulfate (SDS)-polyacrylamide gel electrophoresis (PAGE). After electrophoresis, the samples were transferred to a polyvinylidene difluoride membrane (PVDF), blocked for 2 h with 5% skimmed milk, and incubated with primary antibodies (including anti-PPAR γ , anti-PGC-1 α , anti-UCP1 and anti-GAPDH as a reference gene) at 4°C overnight. After washing three times with tris buffered saline with Tween 20 (TBS-T), the membrane was incubated with a secondary antibody (anti-rabbit IgG) at room temperature. Finally, the proteins were detected using the electrochemiluminescence (ECL) assay, and quantification of the band intensities was performed by Image J software.

Flow cytometric analysis

The differentiated 3T3-L1 cells were collected by trypsinization, washed twice with ice-cold PBS, and then incubated with an antibody cocktail (CD137-APC) for 30 min in the dark. The samples were determined with a BD Fluorescence-Activated Cell Sorting (FACS) AriaTM III Flow Cytometer (BD Biosciences, USA). Flow cytometry data in the form of median fluorescence intensity (MFI) were analyzed and plotted using Flow Jo software.

Statistical analysis

The statistical analysis and graphics were performed using GraphPad Prism 5 (GraphPad Software, USA). All data are expressed as the mean \pm SD, and a comparison was made using one-way ANOVA. Statistical significances between the control and nicotine-treated groups were established at * $P < 0.05$, and ** $P < 0.01$.

RESULTS

Cell viability

The MTT assay revealed that nicotine at concentrations of 10^{-1} to $100 \mu\text{mol/L}$ did not affect cell viability at 24, 48 and 72 h (Fig. 1A-C). Nicotine at a concentration of $10^3 \mu\text{mol/L}$ slightly reduced cell vitality at 72 h ($P < 0.05$), but it did not cause the death of cells. Treatments with 10^4 and $10^5 \mu\text{mol/L}$ nicotine caused a decrease in cell vitality at all three time points ($P < 0.01$). Therefore, the concentration range of 25-100 $\mu\text{mol/L}$ was chosen for further experiments.

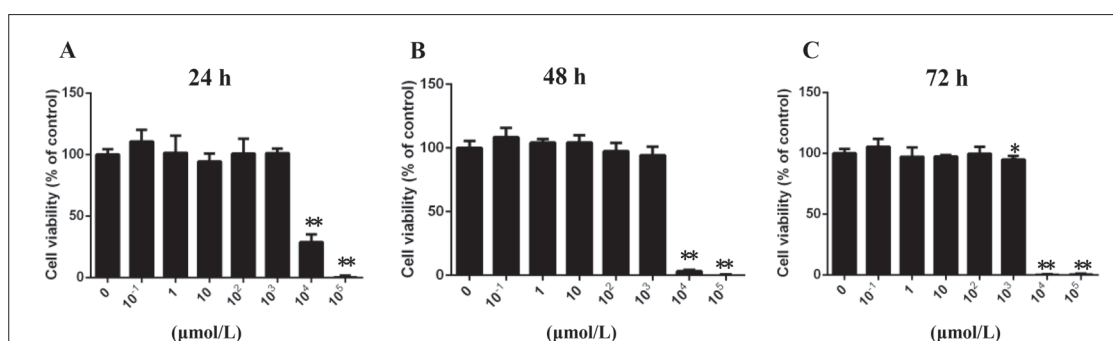


Fig. 1. The effect of nicotine on cell viability at different differentiation stages. 3T3-L1 preadipocytes were seeded onto 96-well plates at a density of 3×10^3 cell/ cm^2 and treated with 10^{-1} - $10^5 \mu\text{mol/L}$ of nicotine for 24 (A), 48 (B) and 72 (C) h. The MTT assay was performed to assess cell viability ($n=8$). ** $P < 0.01$ vs the corresponding controls.

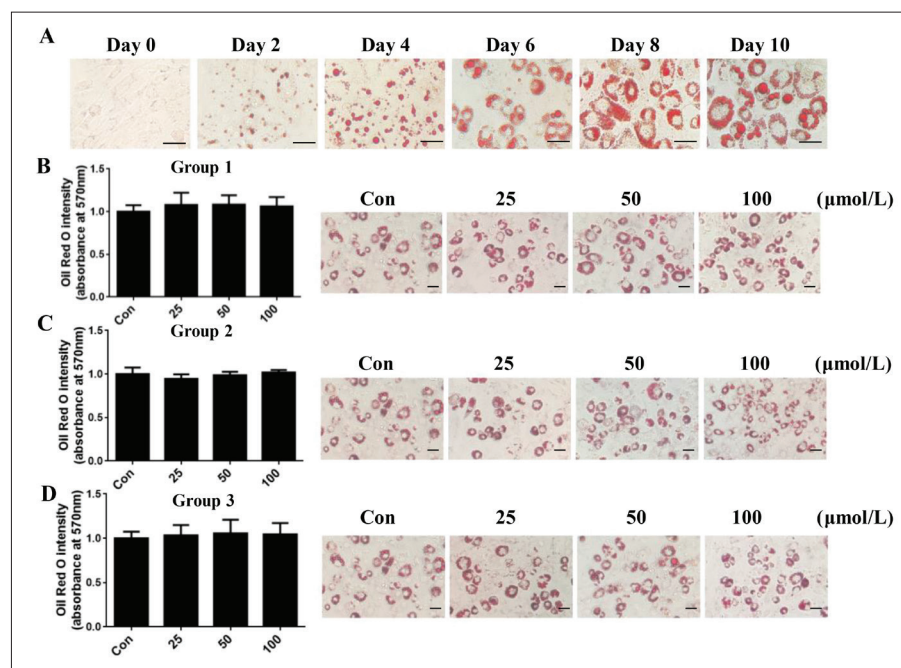


Fig. 2. The effect of nicotine on lipid accumulation at different differentiation stages in 3T3-L1 preadipocytes. **A** – Cells in the process of differentiation were stained with Oil Red O on days 0, 2, 4, 6, 8 and 10 (magnification: 400×). Post-confluent 3T3-L1 preadipocytes were induced to differentiate in Group 1 (**B**), Group 2 (**C**) and Group 3 (**D**). The morphological changes were photographed after Oil Red O staining on day 10 (magnification: 200×). Stained lipids were extracted and quantified by measuring the absorbance at 570 nm. Quantitative data are expressed as means±SD (n=4).

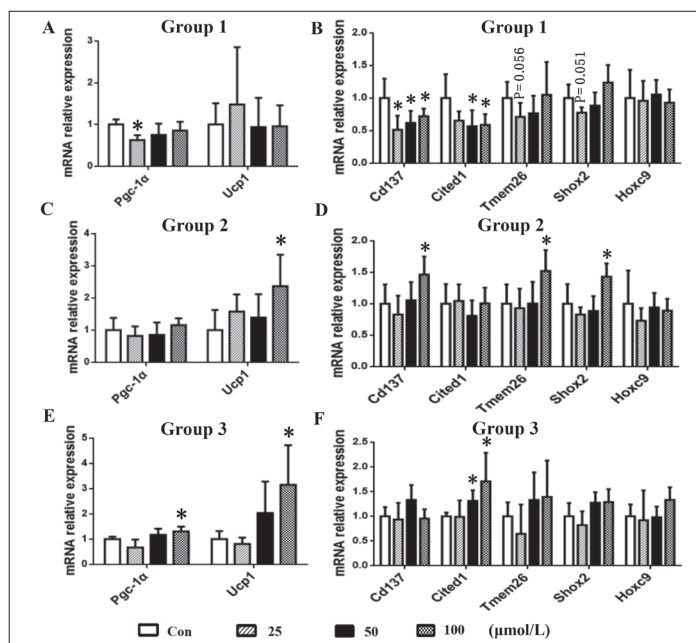


Fig. 3. The effect of nicotine on the gene expression of beige-related genes at different differentiation stages. **A, B** – Nicotine treatment at the early differentiation stage (Group 1, days 0-4); **C, D** – nicotine treatment at the maintenance stage (Group 2, days 5-10); **E, F** – nicotine treatment for 10 days (Group 3, days 0-10). Gene expression of beige-related genes was assessed by RT-qPCR. *Pgc-1α* – peroxisome proliferator-activated receptor gamma coactivator 1-alpha gene; *Ucp1* – uncoupling protein 1 gene; *Cd137* – cluster of differentiation 137 gene; *Cited1* – Cbp/p300 interacting transactivator with Glu/Asp rich carboxy-terminal domain 1 gene; *Tmem26* – transmembrane protein 26 gene; *Shox2* – short stature homeobox 2 gene; *Hoxc9* – homeobox C9 gene. Data are expressed as means±SD (n=5). * $P < 0.05$ vs matching controls.

State of lipid droplets

During the entire differentiation process, the cells were stained with Oil Red O on days 0, 2, 4, 6, 8 and 10 (Fig. 2A). Red lipid droplets began to appear on day 4, and the lipids increased in size from day 4 to day 10. Cells from each group at day 10 were stained with Oil Red O to observe the effect of nicotine on the formation of lipid droplets. Quantitative analysis established that nicotine had little effect on the formation of lipid droplets (Fig. 2B-D).

Nicotine treatment during the early differentiation stage reduced the beige adipocyte-like phenotype in 3T3-L1

In Group 1, treatment with nicotine (25, 50 and 100 $\mu\text{mol/L}$) was from day 0 to day 4. Gene expression of *Pgc-1α* was significantly decreased after exposure to 25 $\mu\text{mol/L}$ nicotine ($P < 0.05$, Fig. 3A). Several beige marker genes, such as *Cd137*, *Tmem26*, *Tbx1*, *Cited1*, *Shox2* and *Hoxc9*, were examined. We found that the gene expression of *Cd137* was significantly decreased in 25, 50 and 100 $\mu\text{mol/L}$ ($P < 0.05$, Fig. 3B). *Cited1* was significantly decreased in 50

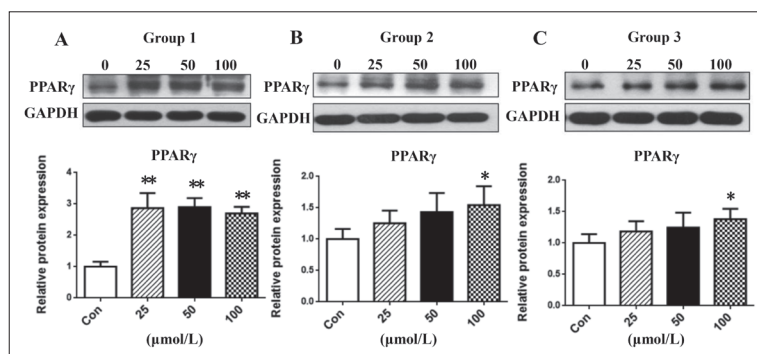


Fig. 4. The effect of nicotine on the protein expression of peroxisome proliferator-activated receptor gamma (PPAR γ) protein at different differentiation stages. **A** – Nicotine treatment at the early differentiation stage (Group 1, days 0-4); **B** – nicotine treatment at the maintenance stage (Group 2, days 5-10); **C** – nicotine treatment for 10 days (Group 3, days 0-10). PPAR γ expression was assessed by Western blotting. Data are expressed as means \pm SD (n=3), with * P <0.05 and ** P <0.01 vs matching controls.

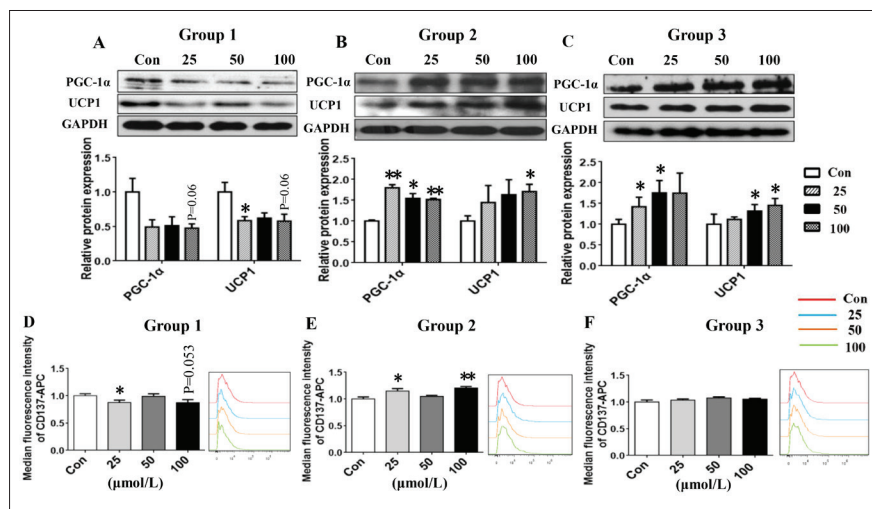


Fig. 5. The effect of nicotine on the protein expression of beige-related genes at different differentiation stages. **A, D** – Nicotine treatment at the early differentiation stage (Group 1, days 0-4); **B, E** – nicotine treatment at the maintenance stage (Group 2, days 5-10); **C, F** – nicotine treatment for 10 days (Group 3, days 0-10). The expression of peroxisome proliferator-activated receptor gamma coactivator 1-alpha (PGC-1 α) protein and uncoupling protein 1 (UCP1) was assessed by Western blotting; cluster of differentiation 137 (CD137) was assessed by flow cytometric analysis. Data are expressed as means \pm SD (n=3). * P < 0.05 and ** P <0.01 vs matching controls.

and 100 μ mol/L (P <0.05, Fig. 3B). Gene expressions of *Tmem26* (P =0.056) and *Shox2* (P =0.051) showed a decreasing trend in the 25 μ mol/L nicotine-exposed group (Fig. 3B). The protein expression of PPAR γ was significantly increased in 25, 50 and 100 μ mol/L (P <0.01, Fig. 4A). Protein expression of PGC-1 α showed a decreasing trend in 100 μ mol/L (P =0.06, Fig. 5A). Protein expression of UCP1 was significantly decreased in 25 μ mol/L (P <0.05, Fig. 5A), exhibiting a decreasing trend in 100 μ mol/L (P =0.06, Fig. 5A). According to the result of the flow cytometric analysis, MFI of CD137-APC was significantly decreased in 25 μ mol/L (P <0.05) and showed a decreasing trend in 100 μ mol/L (P =0.053) (Fig. 5D), which identified decreased protein expression of CD137. The gene and protein expressions of PGC-1 α , UCP1 and CD137 showed a similar downregulated trend when the cells were treated with nicotine at the early differentiation stage.

Nicotine treatment in the later maintenance stage enhanced beige adipocyte-like phenotype in 3T3-L1

In Group 2, nicotine treatment (25, 50, and 100 μ mol/L) was maintained from day 5 to day 10. Gene expression of *Ucp1* was 2.3-fold increased in the 100 μ mol/L nicotine-exposed group (P <0.05, Fig. 3C). Gene expression of *Cd137*, *Tmem26*, and *Shox2* was significantly increased after treatment with 100 μ mol/L nicotine (P <0.05, Fig. 3D). Protein expression of PPAR γ was significantly increased in 100 μ mol/L (P <0.05, Fig. 4B). Protein expression of PGC-1 α was significantly increased in 25 μ mol/L (P <0.01), 50 μ mol/L (P <0.05) and 100 μ mol/L (P <0.01) (Fig. 5B). Protein expression of UCP1 was significantly increased in 100 μ mol/L (P <0.05, Fig. 5B). According to flow cytometric analysis, the MFI of CD137-APC was significantly increased in 25 μ mol/L (P <0.05) and 100 μ mol/L (P <0.01) (Fig.

5E), which identified increased protein expression of CD137. In summary, gene and protein expression of PGC-1 α , UCP1 and CD137 showed a similar upregulated trend when the cells were treated with nicotine at the maintenance stage.

Nicotine treatment during the entire differentiation stage enhanced beige adipocyte-like phenotype in 3T3-L1

In Group 3, nicotine treatment (25, 50 and 100 $\mu\text{mol/L}$) was maintained from day 0 to day 10. Gene expression of *Pgc-1 α* was significantly increased in the 100 $\mu\text{mol/L}$ nicotine-exposed group ($P < 0.05$, Fig. 3E). Gene expression of *Ucp1* was a 3.2-fold increase in the 100 $\mu\text{mol/L}$ nicotine group ($P < 0.05$, Fig. 3E). Both 50 and 100 $\mu\text{mol/L}$ nicotine caused significant increases in *Cited1* ($P < 0.05$, Fig. 3F) gene expression. PPAR γ protein expression was significantly increased in 100 $\mu\text{mol/L}$ -treated cells ($P < 0.05$, Fig. 4C). The expression of PGC-1 α protein at 25 and 50 $\mu\text{mol/L}$ was significantly increased ($P < 0.05$, Fig. 5C), and the expression of UCP1 protein at 50 and 100 $\mu\text{mol/L}$ was significantly increased ($P < 0.05$, Fig. 5C). According to the results of flow cytometric analysis, no significant change was observed in the MFI of CD137-APC (Fig. 5F). In summary, the expression of PGC-1 α , UCP1 and CD137 genes and proteins exhibited similar upregulated trends when the cells were treated with nicotine during the entire differentiation stage.

DISCUSSION

Cigarette smoke is a traditional environmental pollutant, and there are multiple ways of being exposed to it – by active smoking, electronic cigarette smoking, passive smoking, secondhand smoking, third-hand smoking, household smoking and maternal smoking in pregnancy. The exposed population are of diverse gender, age and occupation. Nicotine, the major component of cigarette smoke, is highly liposoluble and accumulates in adipose tissue.

In our study, the chosen doses of nicotine (25, 50 and 100 $\mu\text{mol/L}$) were higher than the serum concentration measured in active smokers. In *in vitro* experiments, the concentration of nicotine ranged from 1 nmol/L to 100 $\mu\text{mol/L}$. In the study of Pei et al. [15], rat fetal hippocampal cell lines were treated with

different concentrations of nicotine (1-100 $\mu\text{mol/L}$). An et al. [16] used 6 nmol/L-60 $\mu\text{mol/L}$ of nicotine in 3T3-L1 cells. Nicotine, a highly lipophilic drug, easily accumulates and has a slow metabolic rate in adipose tissue due to the tissue's small blood flow, which may be responsible for the higher concentrations of nicotine in adipose tissue than in blood [17]. In the normal unstimulated physiological state of adipocytes, the proportion of beige-phenotypic cells is low [18]. *In vitro*, the lack of a regulation mechanism of nerves and hormones in adipocytes may lead to lower beige-like gene and protein expression levels than *in vivo* [19]. Therefore, larger doses are needed in order to observe the functional changes of beige-like adipocytes *in vitro*. According to the results of our MTT assay, 0.1-100 $\mu\text{mol/L}$ nicotine was the safe dose range, and therefore, 0-100 $\mu\text{mol/L}$ nicotine was used.

In our study, the different effects of nicotine on beige adipocyte function were observed depending on cell maturity. When 3T3-L1 cells were treated with nicotine on days 0-4, it mainly acted on embryonic adipocytes *in vivo*. According to Okamatsu-Ogura's study [20], the hypofunction of the beige-like adipocyte function reduced the thermogenesis in adipose tissue, increased fat mass and increased the risk of obesity. Maternal nicotine exposure during pregnancy may act on immature adipocytes in the fetus, and rats whose mothers were treated with nicotine in pregnancy possessed heavier visceral adipose tissue and displayed susceptibility to obesity at 180 days of age [6]. Therefore, it can be speculated that nicotine acting on immature adipocytes (such as in maternal exposure in pregnancy) can decrease fetal beige-like function and lead to obesity susceptibility or metabolic disorder in offspring. However, when nicotine treatment occurred on days 5-10, it mainly acted on mature adipocytes. Nicotine treatment reduced body weight and fat mass, and increased brown adipose tissue thermogenesis in adult rats [3,21]. According to Arai et al. [22], continuous nicotine infusion stimulated UCP1 mRNA expression in the BAT of male adult Wistar rats, and it was speculated that direct nicotine exposure (as in active smoking) activates beige-like function, increases UCP1-induced thermogenesis in adipose tissue, and finally leads to body weight loss. In a related study, although the increase of beige adipocytes showed improvement in obesity, the abnormal increase in beige adipocytes destroyed the energy homeostasis in WAT and could lead to other diseases [23].

We attempted to explain the effect of nicotine on the beige-like phenotype. TLE3 is a white-selective cofactor and PRDM16 is a brown-selective cofactor, both of which determine lipid storage and thermogenic gene programs [24]. According to Santos et al. [25], PPAR γ activation drives both lipogenic or beige-like thermogenic transcriptional programs; PPAR γ and PRDM16 formed a transcriptional complex and induced a beige-like thermogenic program, but PPAR γ , interacting with TLE3, drove a lipid storage transcriptional program [25]. In addition, the increased expression of TLE3 counters PRDM16, suppressing thermogenic genes and inducing white-selective genes, resulting in impaired fatty acid oxidation and thermogenesis [26]. It has been reported that nicotine can enhance PPAR γ expression in adipocytes [2,27]. In our study, nicotine increased the expression of PPAR γ at three different differentiation stages. Therefore, the different effects of nicotine on the beige-like phenotype may be caused by different interactions between PPAR γ and different transcription factors. In Group 1, nicotine mainly acted on preadipocytes. PPAR γ could promote adipogenesis in fibroblasts [28]. In preadipocytes, TLE3, as a cofactor for PPAR γ , regulated adipocyte formation and disrupted the interaction between PPAR γ and PRDM16, which was identified as a key factor in beige adipocytes [29,30]. Therefore, it was inferred that nicotine at the early differentiation stage preferred to promote the formation of the PPAR γ and TLE3 complex rather than the PPAR γ and PRDM16 complex, and inhibited the beige-like phenotype. In Group 2, nicotine mainly acted on differentiated adipocytes. In mature adipocytes, PRDM16 promoted the beige-like phenotype through increased expression of UCP1 [31]. It was reported that PPAR γ interacted with PRDM16 and PGC-1 α and participated in positively regulating the function of the beige-like phenotype in differentiated 3T3-L1 cells [32]. Therefore, it was inferred that nicotine, acting on differentiated adipocytes, preferred to promote the formation of the PPAR γ and PRDM16 complex rather than the PPAR γ and TLE3 complex, further enhancing the beige-like phenotype. In Group 3, the effects of nicotine on the whole cell culture process were similar to those in Group 2 and opposite those in Group 1. It was speculated that the beige-enhancing effects of the PPAR γ and PRDM16 complex at the maintenance stage were stronger than the damaging effects of the PPAR γ and TLE3 complex to beige function at the early differentiation stage. The PPAR γ activation by nicotine

can drive both a lipogenic or beige-like transcriptional program at different differentiation periods, and its roles are most likely associated with nicotine's dual effect on the beige-like phenotype.

CONCLUSION

Exposure of immature adipocytes to nicotine damaged the beige-like phenotype through decreased PGC-1 α and UCP1 expression levels, but nicotine treatment of mature adipocytes or both immature and mature cells enhanced beige-like function through upregulation of PGC-1 α and UCP1. Only a few studies have examined the toxicology of beige adipocytes. Our study focused for the first time on the effects of nicotine on the dysfunction of beige adipocytes. The dual effect of nicotine treatment at different stages *in vitro* is reported for the first time. This mechanism may also provide evidence for the different effects of smoking exposure on adipose tissue from the perspective of the beige adipocyte.

Funding: This work was supported by grants from the National Natural Science Foundation of China (No. 81570792 and 81270950) and from the Large-Scale Instrument and Equipment Sharing Foundation of Wuhan University to You-e Yan.

Author contributions: Hui-jian Chen and Jie Xiang contributed equally to this work. Hui-jian Chen and Jie Xiang conceived, designed, performed the experiments and wrote the manuscript with the guidance of You-e Yan. Wan-xia Zhang, Ao Sun and Gailing Li performed the experiments. The manuscript was edited by Ao Sun and Gai-ling Li. All authors approved of the final version to be published.

Conflict of interest disclosure: The authors declare no conflict of interest.

REFERENCES

1. Wipfli HL, Samet JM. Second-hand smoke's worldwide disease toll. *Lancet*. 2011;377(9760):101-2.
2. Somm E, Schwitzgebel VM, Vauthay DM, Camm EJ, Chen CY, Giacobino JP, Sizonenko SV, Aubert ML, Huppi PS. Prenatal nicotine exposure alters early pancreatic islet and adipose tissue development with consequences on the control of body weight and glucose metabolism later in life. *Endocrinology*. 2008;149(12):6289-99.
3. Liu M, Chuang Key CC, Weckerle A, Boudyguina E, Sawyer JK, Gebre AK, Spoo W, Makwana O, Parks JS. Feeding of tobacco blend or nicotine induced weight loss associated with decreased adipocyte size and increased physical activity in male mice. *Food Chem Toxicol*. 2018;113:287-95.

4. Kim SH, Plutzky J. Brown Fat and Browning for the Treatment of Obesity and Related Metabolic Disorders. *Diabetes Metab J*. 2016;40(1):12-21.
5. Wu J, Bostrom P, Sparks LM, Ye L, Choi JH, Giang AH, Khandekar M, Virtanen KA, Nuutila P, Schaart G, Huang K, Tu H, van Marken Lichtenbelt WD, Hoeks J, Enerback S, Schrauwen P, Spiegelman BM. Beige adipocytes are a distinct type of thermogenic fat cell in mouse and human. *Cell*. 2012;150(2):366-76.
6. Gao YJ, Holloway AC, Zeng ZH, Lim GE, Petrik JJ, Foster WG, Lee RM. Prenatal exposure to nicotine causes postnatal obesity and altered perivascular adipose tissue function. *Obes Res*. 2005;13(4):687-92.
7. Yoshida T, Sakane N, Umekawa T, Kogure A, Kondo M, Kumamoto K, Kawada T, Nagase I, Saito M. Nicotine induces uncoupling protein 1 in white adipose tissue of obese mice. *Int J Obes Relat Metab Disord*. 1999;23(6):570-5.
8. Green H, Meuth M. An established pre-adipose cell line and its differentiation in culture. *Cell*. 1974;3(2):127-33.
9. An Z, Wang H, Song P, Zhang M, Geng X, Zou MH. Nicotine-induced activation of AMP-activated protein kinase inhibits fatty acid synthase in 3T3L1 adipocytes: a role for oxidant stress. *J Biol Chem*. 2007;282(37):26793-801.
10. Bai XJ, Fan LH, He Y, Ren J, Xu W, Liang Q, Li HB, Huo JH, Bai L, Tian HY, Fan FL, Ma AQ. Nicotine may affect the secretion of adipokines leptin, resistin, and visfatin through activation of KATP channel. *Nutrition*. 2016;32(6):645-8.
11. Lone J, Parray HA, Yun JW. Nobiletin induces brown adipocyte-like phenotype and ameliorates stress in 3T3-L1 adipocytes. *Biochimie*. 2018;146:97-104.
12. Puigserver P, Wu Z, Park CW, Graves R, Wright M, Spiegelman BM. A cold-inducible coactivator of nuclear receptors linked to adaptive thermogenesis. *Cell*. 1998;92(6):829-39.
13. Sharp LZ, Shinoda K, Ohno H, Scheel DW, Tomoda E, Ruiz L, Hu H, Wang L, Pavlova Z, Gilsanz V, Kajimura S. Human BAT possesses molecular signatures that resemble beige/brite cells. *PloS One*. 2012;7(11):e49452.
14. Lidell ME, Betz MJ, Dahlqvist Leinhard O, Heglind M, Elander L, Slawik M, Mussack T, Nilsson D, Romu T, Nuutila P, Virtanen KA, Beuschlein F, Persson A, Borga M, Enerback S. Evidence for two types of brown adipose tissue in humans. *Nat Med*. 2013;19(5):631-4.
15. Pei Y, Jiao Z, Dong W, Pei L, He X, Wang H, Xu D. Excitotoxicity and compensatory upregulation of GAD67 in fetal rat hippocampus caused by prenatal nicotine exposure are associated with inhibition of the BDNF pathway. *Food Chem Toxicol*. 2019; 123:314-25.
16. An Z, Wang H, Song P, Zhang M, Geng X, Zou MH. Nicotine-induced activation of AMP-activated protein kinase inhibits fatty acid synthase in 3T3L1 adipocytes: a role for oxidant stress. *J Biol Chem*. 2007; 282(37):26793-801.
17. La Merrill M, Emond C, Kim MJ, Antignac JP, Le Bizet B, Clement K, Birnbaum LS, Barouki R. Toxicological function of adipose tissue: focus on persistent organic pollutants. *Environ Health Perspect*. 2013;121(2):162-9.
18. Harms M, Seale P. Brown and beige fat: development, function and therapeutic potential. *Nat Med*. 2013;19(10):1252-63.
19. Asano H, Kanamori Y, Higurashi S, Nara T, Kato K, Matsui T, Funaba M. Induction of beige-like adipocytes in 3T3-L1 cells. *J Vet Med Sci*. 2014; 76(1):57-64.
20. Okamatsu-Ogura Y, Fukano K, Tsubota A, Uozumi A, Terao A, Kimura K, Saito M. Thermogenic ability of uncoupling protein 1 in beige adipocytes in mice. *PloS One*. 2013;8(12):e84229.
21. Seoane-Collazo P, Martinez de Morentin PB, Ferno J, Dieguez C, Nogueiras R, Lopez M. Nicotine improves obesity and hepatic steatosis and ER stress in diet-induced obese male rats. *Endocrinology*. 2014;155(5):1679-89.
22. Arai K, Kim K, Kaneko K, Iketani M, Otagiri A, Yamauchi N, Shibasaki T. Nicotine infusion alters leptin and uncoupling protein 1 mRNA expression in adipose tissues of rats. *Am J Physiol Endocrinol Metab*. 2001;280(6):E867-76.
23. Zhang H, Zhu L, Bai M, Liu Y, Zhan Y, Deng T, Yang H, Sun W, Wang X, Zhu K, Fan Q, Li J, Ying G, Ba Y. Exosomal circRNA derived from gastric tumor promotes white adipose browning by targeting the miR-133/PRDM16 pathway. *Int J Cancer*. 2019;144(10):2501-15.
24. Villanueva CJ, Waki H, Godio C, Nielsen R, Chou WL, Vargas L, Wroblewski K, Schmedt C, Chao LC, Boyadjian R, Mandrup S, Hevener A, Saez E, Tontonoz P. TLE3 is a dual-function transcriptional coregulator of adipogenesis. *Cell Metab*. 2011;13(4):413-27.
25. Santos GM, Neves Fde A, Amato AA. Thermogenesis in white adipose tissue: An unfinished story about PPARgamma. *Biochim Biophys Acta*. 2015;1850(4):691-5.
26. Villanueva CJ, Vergnes L, Wang J, Drew BG, Hong C, Tu Y, Hu Y, Peng X, Xu F, Saez E, Wroblewski K, Hevener AL, Reue K, Fong LG, Young SG, Tontonoz P. Adipose subtype-selective recruitment of TLE3 or Prdm16 by PPARγ specifies lipid storage versus thermogenic gene programs. *Cell Metab*. 2013; 17(3):423-35.
27. Wang Z, Wang D, Wang Y. Cigarette Smoking and Adipose Tissue: The Emerging Role in Progression of Atherosclerosis. *Mediators Inflamm*. 2017;2017:3102737.
28. Tontonoz P, Hu E, Spiegelman BM. Stimulation of adipogenesis in fibroblasts by PPAR gamma 2, a lipid-activated transcription factor. *Cell*. 1994;79(7):1147-56.
29. Seale P, Bjork B, Yang W, Kajimura S, Chin S, Kuang S, Scime A, Devarakonda S, Conroe HM, Erdjument-Bromage H, Tempst P, Rudnicki MA, Beier DR, Spiegelman BM. PRDM16 controls a brown fat/skeletal muscle switch. *Nature*. 2008;454(7207):961-7.
30. Kokabu S, Lowery JW, Jimi E. Cell Fate and Differentiation of Bone Marrow Mesenchymal Stem Cells. *Stem Cells Int*. 2016;2016:3753581.
31. Subash-Babu P, Alshatwi AA. Ononitol monohydrate enhances PRDM16 & UCP-1 expression, mitochondrial biogenesis and insulin sensitivity via STAT6 and LTB4R in maturing adipocytes. *Biomed Pharmacother*. 2018;99:375-83.
32. Mu Q, Fang X, Li X, Zhao D, Mo F, Jiang G, Yu N, Zhang Y, Guo Y, Fu M, Liu JL, Zhang D, Gao S. Ginsenoside Rb1 promotes browning through regulation of PPARgamma in 3T3-L1 adipocytes. *Biochem Biophys Res Commun*. 2015;466(3):530-5.

Supplementary Data

Supplementary Table S1

Available at: http://serbiosoc.org.rs/NewUploads/Uploads/Chen%20et%20al_4148_Supplementary%20Table%20S1.pdf